Volume 8, Issue 6, 2018, 3719 - 3724 **ISSN 2069-5837**

Biointerface Research in Applied Chemistry

www.BiointerfaceResearch.com

Original Research Article **Open Access Journal**

Received: 18.10.2018 / Revised: 03.12.2018 / Accepted: 10.12.2018 / Published on-line: 15.12.2018

Molecular modeling analyses of polyaniline substituted with alkali and alkaline earth elements

Rania Badry [1], Hassanein Shaban [2], Hanan Elhaes [3], Ahmed Refaat [4], Medhat Ibrahim [4]

[1]Physics Department, Faculty of Women for Arts, Science and Education, Ain Shams University, 11757 Cairo, Egypt
[2]Physics Department, Biophysics Branch, Faculty of Science, Ain Shams University, 11566, Cairo, Egypt
[3]Spectroscopy Department, National Research Centre, 33 El-Bohouth Str. 12622 Dokki, Giza, Egypt

*corresponding author e-mail address: ***medahmed6@yahoo.com,***

ABSTRACT

Polyaniline which is termed as PANi is chosen as model molecule where substitution with Li, Na, K, Be, Mg and Ca is carried out. Each metal is supposed to interact with PANi throughout the amide group at the terminal and then in the middle of PANi. Quantum mechanical calculations at B3LYP/6-31G (d,p) level are conducted for PANi as well as substituted PANi. Bond distances, bond angles, total dipole moment (TDM), frontier band gap energy (HOMO/LUMO) as well as molecular electrostatic potential (ESP) are calculated. Results indicate that for terminal amide group interaction, PANi-Na has the highest TDM (10.5996 Debye) and the lowest HOMO/LUMO band gap energy (2.0169 eV). Also for PANi-Ca, TDM (6.4356 Debye); HOMO/LUMO (1.1970 eV). For the interaction through the middle NH group, PANi-K and PANi-Mg are the more active sites for interaction as they have the highest TDM, having the values of 11.5939 and 3.1208 Debye respectively, and the lowest HOMO/LUMO band gap energies of 1.6732 and 1.3168 eV respectively. ESP drives a general conclusion that the electronegativity of PANi increases significantly by the presence of alkali metals and increases slightly by the presence of alkaline earth metals. Additionally, there are changes in the geometrical parameters (including both bond lengths and bond angles) for all studied model molecules.

Keywords: *PANi; B3LYP/6-31G (d,p); HOMO/LUMO; Total dipole moment; Electrostatic potential; Geometrical parameters.*

1. INTRODUCTION

Polyaniline which is termed PANi is a semi-flexible rod polymer belonging to conducting polymer, and since its discovery it is among the most studied polymers [1-2]. The wide applications of PANi are due to its good environmental stability, controllable electrical properties and high conductivity [3-4]. Structural aspects in polyanilines continue to be an interesting research topic [5-7]. Nevertheless, the number of papers dealing with the structural properties of Polyaniline Emeraldine-base form (EB-PANi), which is the starting point for all further treatments, is still rather low [8-10]. PANi among other conducting polymers shows excellent properties for some applications including energy storage, sensors and electrochromic devices. PANi shows more attention as compared with its family of conducting polymers as it possesses the highest specific capacitance according to many technical reasons such as thermal stability, multi-redox reactions and good electronic properties due to protonation, besides other non-technical reasons such as the low cost for its infinite abundance [11-12]. A survey is conducted to indicate that PANi is a promising tool for electrode materials for energy storage and conversion [13]. PANi is modified in nano form to act as a sensor for formaldehyde [14]. For enhancing its properties, a composite is made from PANi and multiwall carbon nanotubes [15]. Further enhancement of PANi to be applied in supercapacitor applications is to prepare Fe-doped PANi/sulfonated carbon nanotubes [16]. Recently, PANi is a hot topic of research as it is applied in the nano form with other structures for modern applications including, PANi/carbon nanofiber as electroconductive materials [17]. PANi is modified with cotton to act as a sensor for H_2S [18]. A composite of PANi/bismuth is shown to have enhanced thermoelectric performance [19]. Modified PANi with carbon nanomaterials as well as other nanocomposites show potential application in the field of energy storage materials dedicating them for devices; these can be met with supercapacitors, which complement batteries [20-23]. The suitability of PANi in the field of energy storage materials and application is that its ability to store and release energy through redox processes [24-26].

In this work, PANi and PANi substituted with Li, Na, K, Be, Mg and Ca are calculated at B3LYP/6-31G (d,p) level. Metals are interacted with PANi through the amide group at the terminal and then in the middle of PANi. The total dipole moment (TDM), highest occupied and the lowest unoccupied molecular orbits (HOMO/LUMO) band gap energy, molecular electrostatic potential (ESP) and geometrical parameters were calculated.

2. EXPERIMENTAL SECTION

Calculation Details.

Model molecules were designed for PANi and PANi interacted with alkali metals such as Li, Na and K, and with alkaline earth metals like Be, Mg and Ca. Calculations were accomplished with personal computer at Spectroscopy Department, National Research Centre, Egypt using Gaussian 09 program [27]. All the

studied molecules underwent optimization with density functional theory (DFT) quantum mechanical calculations at B3LYP/6-31G (d,p) basis set [28-30]. The TDM, HOMO/LUMO band gap energy, ESP and geometrical parameters are calculated for each model.

3. RESULTS SECTION

Model molecules representing PANi and PANi substituted with alkali metals (Li, Na and K) and with alkaline earth metals (Be, Mg and Ca) are indicated in figure 1 and figure 2 respectively. For all studied structures, metals are assumed to interact with PANi through the hydrogen of the terminal amide group (as indicated in figure 1-a,b,c,d,e,f,g) and then through the hydrogen of the amide group located in the middle of the model molecule (as indicated in figure 2-a,b,c,d,e,f). There is only one mechanism of interaction, which is a complex state.

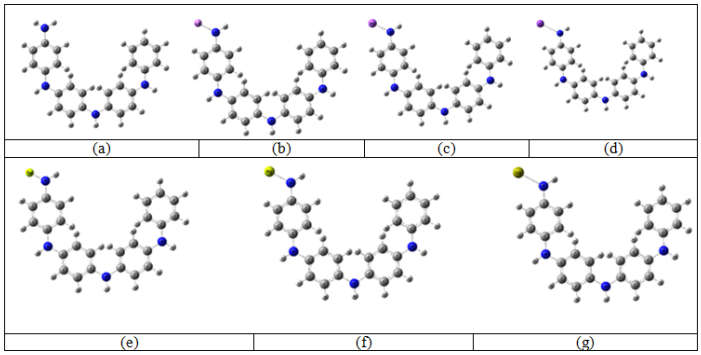

Figure 1. B3LYP/6-31G (d,p) optimized structures of a: PANi, b: PANi-Li, c: PANi-Na, d: PANi-K, e: PANi-Be, f: PANi-Mg and g: PANi-Ca throughout terminal amide group.

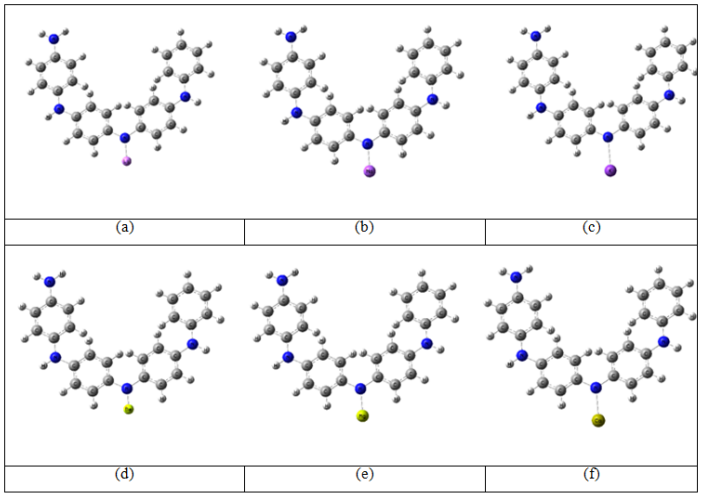

Figure 2. B3LYP/6-31G (d,p) optimized structures of a: PANi -Li, b: PANi-Na, c: PANi-K, d: PANi-Be, e: PANi-Mg and f: PANi-Ca through middle NH group.

It is stated earlier that the TDM and HOMO/LUMO band gap energy reflect the reactivity of a given chemical structure [31,32]. The calculated TDM as Debye and HOMO/LUMO band gap energy (ΔE) as eV are calculated at B3LYP/6-31G (d,p).

Table 1 exhibits the TDM and HOMO/LUMO band gap energy for PANi and PANi-Li, PANi-Na, PANi-K, PANi-Be, PANi-Mg and PANi-Ca through interaction with the terminal amide group. The HOMO/LUMO of the same structures are illustrated in figure 3-a,b,c,d,e,f,g. As a result of the interaction, it is found that in case of terminal interaction, TDM increased by the substitution of hydrogen atom of the amide group with Li, Na, K, Be, Mg and Ca while HOMO/LUMO band gap energy highly decreased. By substitution, TDM increased from 2.5408 Debye to 10.5996 Debye and HOMO/LUMO band gap energy decreased from 4.1500 eV to 2.0169 eV. From our study, we noticed that in case of terminal interaction, the increase of TDM after interaction with alkali metals is higher than that with alkaline earth metals, such that the TDM after interaction with Li, Na and K is higher than that with Be, Mg and Ca; however, the decrease in HOMO/LUMO band gap energy of alkaline earth metals is higher than that of alkali metals, such that the HOMO/LUMO band gap energy of Li, Na and K is higher than that of Be, Mg and Ca. In case of alkali metals, the highest TDM and lowest HOMO/LUMO band gap energy are those for PANi-Na, while in case of alkaline earth metals, the highest TDM is that for PANi-Ca but the lowest HOMO/LUMO band gap energy is that for PANi-Mg. Figures 3 and 4 present the HOMO/LUMO band gap energy for PANi and PANi-Li, PANi-Na, PANi-K, PANi-Be, PANi-Mg and PANi-Ca through terminal amide group and middle NH group respectively.

Table 1. B3LYP/6-31G (d,p) calculated total dipole moment (TDM) as Debye; HOMO-LUMO band gap energy (ΔE) as eV for the studied structures: PANi, PANi-Li, PANi-Na, PANi-K, PANi-Be, PANi-Mg and PANi-Ca through terminal amide group.

Structure	TDM	ΔE
PANi	2.5408	4.1500
PANi-Li	10.2356	2.1470
PANi-Na	10.5996	2.0169
PANi-K	6.4953	2.1277
PANi-Be	1.5523	2.6795
PANi-Mg	3.7819	1.1391
PANi-Ca	6.4356	1.1970

Table 2 displays the TDM and HOMO/LUMO band gap energy for PANi-Li, PANi-Na, PANi-K, PANi-Be, PANi-Mg and PANi-Ca through the middle NH group. HOMO/LUMO band gap energy is indicated in figure 4-a,b,c,d,e,f. In case of middle NH group interaction and as in the case of terminal interaction, TDM increased by substitution of the hydrogen atom of the NH group with the studied metals and HOMO/LUMO band gap energy significantly decreased. TDM increased up to 11.5939 Debye while HOMO/LUMO band gap energy decreased to 1.6468 eV. Additionally, the increase in TDM of alkali metals is higher than that of alkaline earth metals, such that the TDM of Li, Na and K is higher than that of Be, Mg and Ca as in the case of terminal interaction. In case of interaction of the middle NH group with alkali metals, the highest TDM equals 11.5939 Debye which is for PANi-K and the lowest HOMO/LUMO band gap energy equals 1.6468 eV for PANi-Na. The highest TDM for alkaline earth metals equals 5.3334 Debye for PANi-Ca and the lowest HOMO/LUMO band gap energy equals 1.3168 eV for PANi-Mg.

Another indication for the reactivity of the given structures is indicated with molecular ESP. As indicated earlier, it is a measure for the points through which each structure is going to interact with the surrounding structures [33-35].

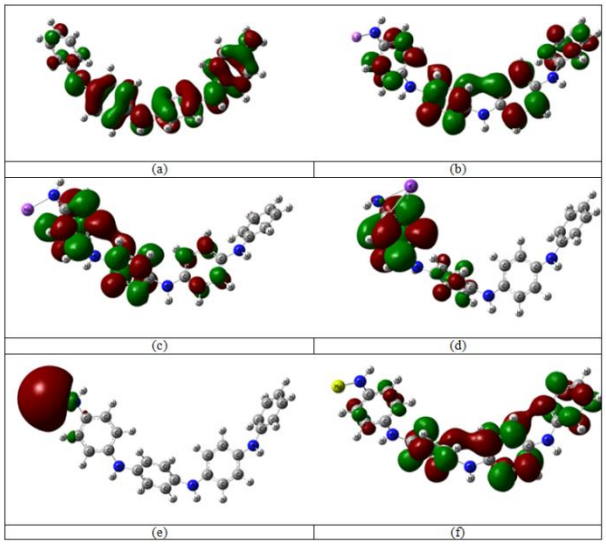

Figure 3. B3LYP/6-31G (d,p) HOMO/LUMO band gap energy of a: PANi, b: PANi-Li, c: PANi-Na, d: PANi-K, e: PANi-Be, f: PANi-Mg and g: PANi-Ca through terminal amide group.

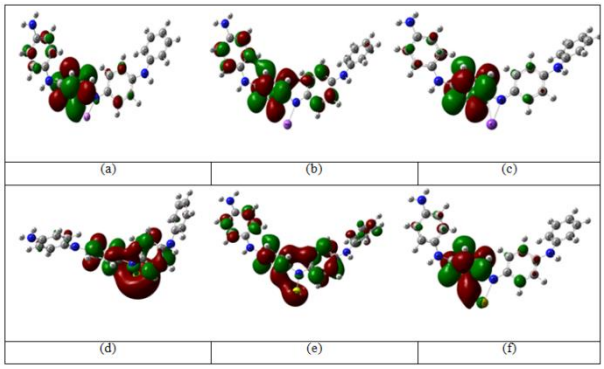

Figure 4. B3LYP/6-31G (d,p) HOMO/LUMO band gap energy of a: PANi-Li, b: PANi-Na, c: PANi-K, d: PANi-Be, e: PANi-Mg and f: PANi-Ca through middle NH group.

Table 2. B3LYP/6-31G (d,p)calculated total dipole moment (TDM) as Debye; HOMO-LUMO band gap energy (ΔE) as eV for the studied structures: PANi-Li, PANi-Na, PANi-K, PANi-Be, PANi-Mg and PANi-Ca through middle NH group.

Structure	TDM	ΔE
PANi-Li	6.9552	2.5062
PANi-Na	9.4663	1.6468
PANi-K	11.5939	1.6732
PANi-Be	3.4601	3.0823
PANi-Mg	3.1208	1.3168
PANi-Ca	5.3334	1.4569

ESP was also calculated at the same level of theory for all structures under investigation. ESP is drawn as contour then as total surface area for all structures. Figures 5 and 6 illustrate the ESP as contour action for all model molecules in the two schemes of interaction (terminal and middle) respectively. Also, ESP study depicts the reactivity of a given structure. As shown in figures 5 and 6, the electronegativity of PANi highly increased by the presence of alkali metals and slightly increased by the presence of alkaline earth metals. Figures 7 and 8 present the ESP for the same structures as total surface area.

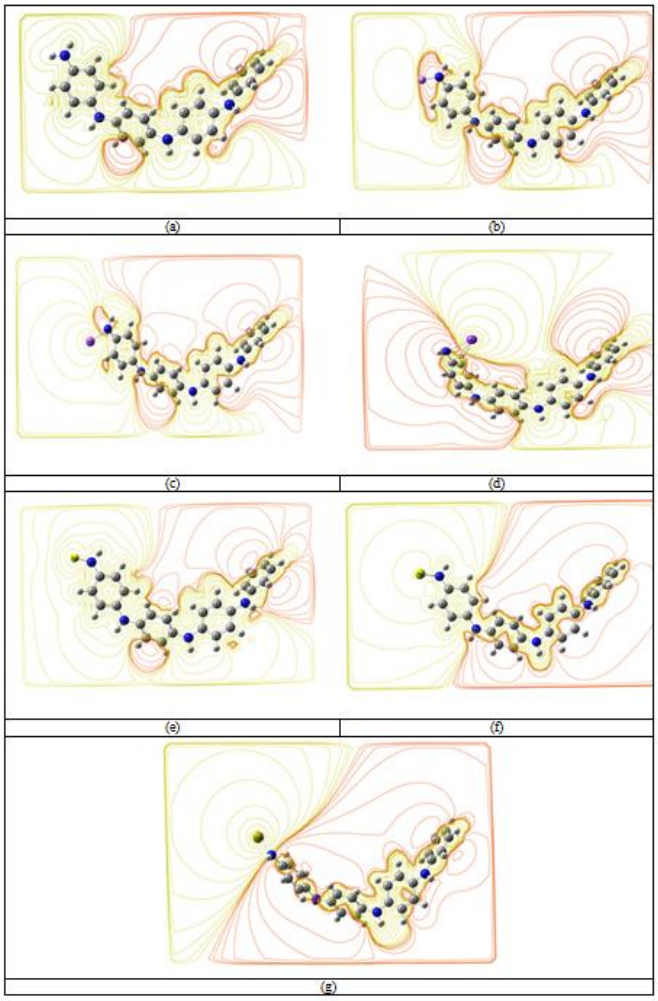

Figure 5. B3LYP/6-31G (d,p) ESP as contour of a: PANi, b: PANi-Li, c: PANi-Na, d: PANi-K, e: PANi-Be, f: PANi-Mg and g: PANi-Ca through terminal amide group.

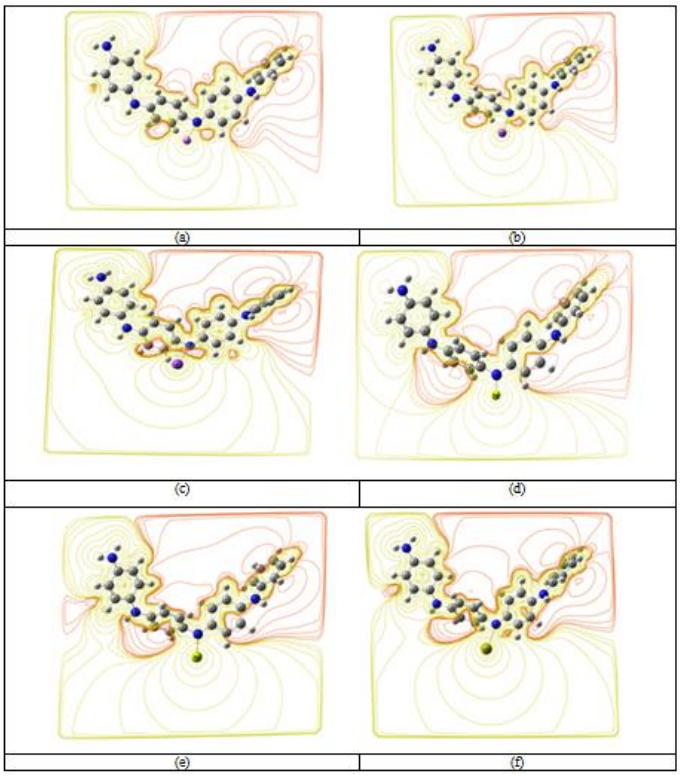

Figure 6. B3LYP/6-31G (d,p) ESP as contour of a: PANi-Li, b: PANi-Na, c: PANi-K, d: PANi-Be, e: PANi-Mg and f: PANi-Ca through middle NH group.

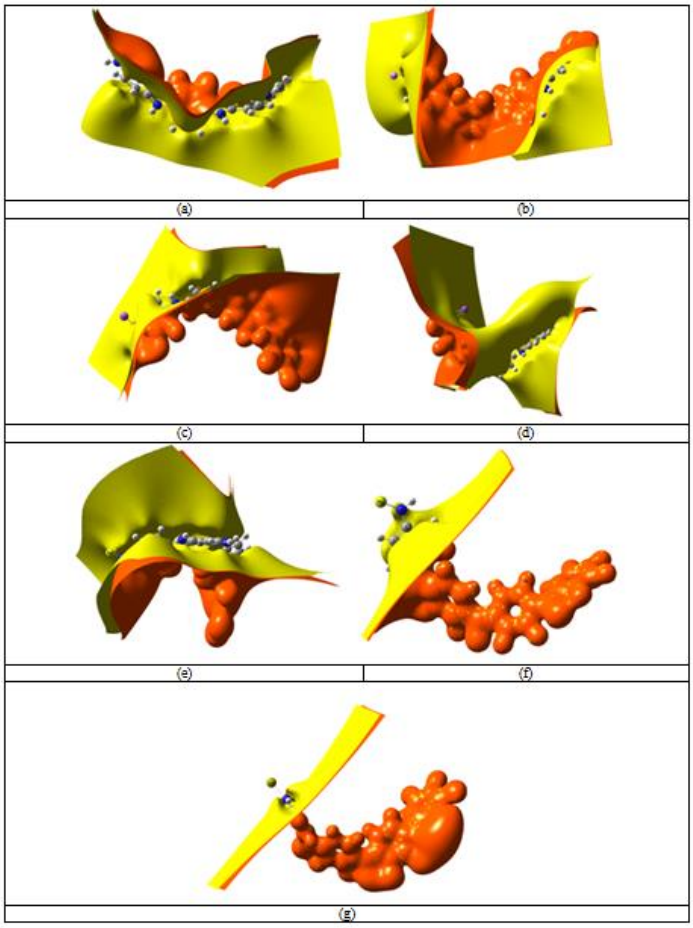

Figure 7. B3LYP/6-31G (d,p) ESP as a total surface of a: PANi, b: PANi-Li, c: PANi-Na, d: PANi-K, e: PANi-Be, f: PANi-Mg and g: PANi-Ca through terminal amide group.

Table 3 illustrates the influence of interaction between the different groups of metals with PANi which produces a change in both bond length and bond angle for all studied models. The bond length in both cases of interaction with the terminal amide group increased from 1.01172 Å to 2.54357 Å from Li to K, and to 2.30093 Å from Be to Ca. On the other hand, the bond angles for terminal interaction are also influenced where there are two angles involved which are X50N2H49 and X50N2C3. When PANi interacted with Li, Na, K, Be, Mg and Ca, the values of bond angles are larger than that of PANi itself for the angle X50N2H49 where X=Li, Na, K, Be, Mg and Ca, but for the angle X50N2C3, the bond angles changed from 114.166° to 127.102°, 92.862°, 93.281°, 133.478°, 128.626° and 126.537° for Li, Na, K, Be, Mg and Ca respectively. For the middle NH group, the bond length increased from 1.00836 Å to 2.56133 Å and 2.34490 Å for alkali metals and alkaline earth metals respectively. There are also two angles included when the interaction proceeds through the middle NH group which are X50N22C16 and X50N22C25. The bond angle of X50N22C16 decreased from 115.491° to 84.391°, 91.040°, 89.515°, 113.917°, 112.384° and 93.748° for Li, Na, K, Be, Mg and Ca respectively, but for angle X50N22C25 it increased from 115.383° to 145.068°, 141.034°, 130.441°, 126.828°, 126.806° and 140.193° for Li, Na, K, Be, Mg and Ca respectively.

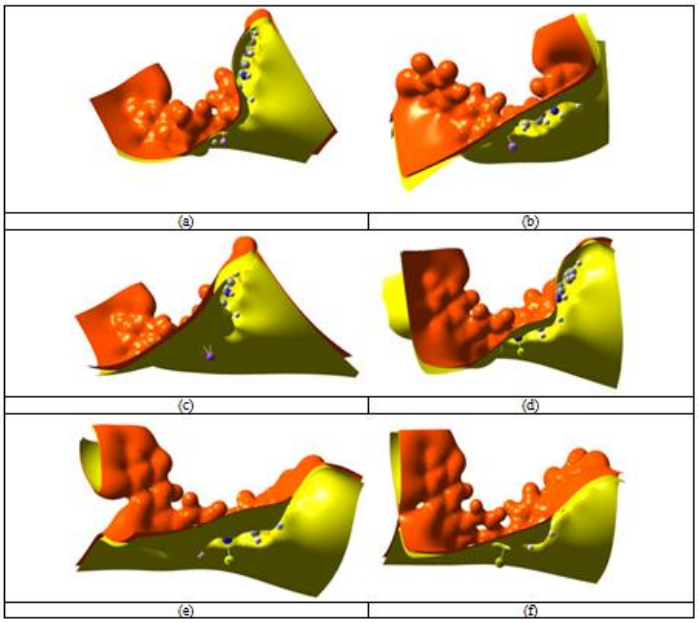

Figure 8. B3LYP/6-31G (d,p) ESP as a total surface of a: PANi-Li, b: PANi-Na, c: PANi-K, d: PANi-Be, e: PANi-Mg and f: PANi-Ca through middle amide group.

Table 3. B3LYP/6-31G (d,p) calculated bond length and bond angle for all studied structures: PANi , PANi -Li, PANi -Na, PANi - K, PANi -Be, PANi -Mg and PANi -Ca throughout both hydroxyl group and middle NH group where X=H, Li, Na, K, Be, Mg and Ca respectively .

Structure	Bond length		Bond angle			
	Terminal NH2 (N2X50)	Middle NH (N22-X50)	Terminal NH		Middle NH	
			(X50N2H49)	(X50N2C3)	(X50N22C16)	(X50N22C25)
PANi	1.01172	1.00836	110.706	114.166	115.491	115.383
PANi-Li	1.78961	1.82598	123.438	127.102	84.391	145.068
PANi-Na	2.16015	2.18075	135.896	92.862	91.040	141.034
PANi-K	2.54357	2.56133	131.171	93.281	89.515	130.441
PANi-Be	1.51660	1.52720	115.547	133.478	113.917	126.828
PANi-Mg	1.95842	1.97700	118.148	128.626	112.384	126.806
PANi-Ca	2.30093	2.34490	123.879	126.537	93.748	140.193

4. CONCLUSIONS

Molecular modeling generally shows potential to study all classes of polymers as it is applied for synthetic polymers in this work and previously applied for natural polymers (36-38). Additionally, DFT level of theory proves to be effective in studying and following up the structural and electronic properties

of PANi and is in a good agreement with previous work applied for different other materials (39-43).

DFT computational analyses for PANi, and PANi substituted with alkali metals and alkaline earth metals at the terminal and middle amide groups indicated the following. In case of terminal amide group interaction, PANi-Na has the highest TDM and lowest HOMO/LUMO band gap energy equal 10.5996 Debye and 2.0169 eV respectively, indicating that sodium is the most active metal from all alkali metals studied, and also PANi-Ca with the TDM and HOMO/LUMO values of 6.4356 Debye and 1.1970 eV respectively is the most active in comparison with all the studied alkaline earth metals. When the interaction was done via the middle NH group through the chain, PANi-K and PANi-Mg are the most active metals for interaction as they have the highest TDM values of 11.5939 and 3.1208 Debye respectively, and the lowest HOMO/LUMO band gap energy values of 1.6732 and 1.3168 eV respectively.

ESP indicated that generally the electronegativity of PANi is increased significantly by the presence of alkali metals and increased slightly by the presence of alkaline earth metals. The changes in both bond lengths and bond angles upon optimization also reflect the reactivity of PANi upon interaction with the studied metals which is in agreement with the results of TDM, HOMO/LUMO band gap energy and ESP.

5. REFERENCES

[1] Yoshikuko O., Walter B., Ch.7: Organic, Semiconductors, *Polymers. Reinhold*, 125-158, **1964**.

[2] Alan H., Nobel Lecture: Semiconducting and metallic polymers: The fourth generation of polymeric materials, *Reviews of Modern Physics*, 73 3, 681, **2001**.

[3] Park S.Y., Cho M.S., Choi H.J., Synthesis and electrical characteristics of polyaniline nanoparticles and their polymeric composite, *Curr. Appl. Phys.*, 4, 581-583, **2004**.

[4] Sanches E. A., Soares J. C., Mafud A.C., Fernandes E.G.R., Leite F.L., Mascarenhas Y.P., Structural characterization of Chloride Salt of conducting polyaniline obtained by XRD, SAXD, SAXS and SEM, *J. Mol. Struct*., 1036, 121-126, **2013**.

[5] Józefowicz M.E., Epstein A.J., Pouget J.P., Masters J.G., Ray A., Sun Y., Tang X., Macdiarmid A.G., X-ray structure of polyanilines, *Synth.Metals*, 41- 43, 723-726, **1991**.

[6] Sanches E.A., Soares J.C., Iost R.M., Marangoni V.S., Trovati G., Batista T., Mafud A.C., Zucolotto V., Mascarenhas Y.P., Structural characterization of emeraldine-salt polyaniline/gold nanoparticles complexes, *J. Nanomater*., 1, 1, **2011**.

[7] Sanches E.A., Soares J.C., Mafud A.C., Trovati G., Fernandes E.G., Mascarenhas Y.P., Structural and morphological characterization of chloride salt of conducting poly(o-methoxyaniline) obtained at different time synthesis, *J. Mol. Struct*., 1039, 167-173, **2013**.

[8] Luźny W., Śniechowski M., The role of water content for the emeraldine base structure, *Fibres & Text. East. Eur*., 11(5), 75-79, **2003**.

[9] Ibrahim M., Koglin E., Spectroscopic Study of PolyanilineEmeraldine Base: Modelling Approach, *Acta. Chim. Slov*., 52, 159-163, **2005**.

[10] Bhadra S., Khastgir D., Singha N.K., Lee J.H., Progress in preparation, processing and applications of polyaniline, *Prog. Polym. Sci.*, 34, 783-810, **2009.**

[11] Snook G.A., Kao P., Best A.S., Conducting-polymer-based supercapacitor devices and electrodes, *J. Power Sources*, 196, 1-12, **2011.**

[12] Silva C.H., Galiote N.A., Huguenin F., Teixeira-Neto É., Constantino V.R., Temperini M.L., Spectroscopic morphological and electrochromic characterization of layer-by-layer hybrid films of polyaniline and hexaniobatenanoscrolls, *J. Mater. Chem.*, 22, 14052-14060, **2012.**

[13] Wang H., Wang H., Shenm Z.X., Polyaniline (PANi) based electrode materials for energy storage and conversion, *J. of Science: Advanced Materials and Devices*, 1, 225-255, **2016.**

[14] Omara W., Amin R., Elhaes H., Ibrahim M., Elfeky S.A., Preparation and Characterization of Novel PolyanilineNanosensor for Sensitive Detection of Formaldehyde, *Recent. Pat..Nanotech*., 9, 195-203, **2015.**

[15] Khalil M.H., El-Enany G.M., El-Khodary S.A., El-Okr M., Ibrahim M., On the Spectroscopic Analyses of Polyaniline/Multiwalled Carbon Nanotube, *Der PharmaChem*., 8, 1, 1-5, **2016**.

[16] El-Khodary S.A., El-Enany G.M., El-Okr Ibrahim M., Modified Iron Doped Polyaniline/Sulfonated Carbon Nanotubes for All Symmetric Solid-State Supercapacitor, *Synth. Met*., 233, 41-51, **2017**.

[17] Rusen E., Diacon A., Damian C., Gavrila R., Dinescu A., Dumitrescu A., Zecheru T., Electroconductive materials based on carbon nanofibers and polyaniline, *J. Appl. Polym. Sci*., 135, 46873, 1-7, **2018.**

[18] Almeida T.M., Maranhão F.S., Carvalho F.V., Middea A., Araujo J.R., Júnior F.G.S., H2S Sensing Material Based on Cotton Fabrics Modified with Polyaniline, *Macromol.Symp*., 381,1800111, **2018.**

[19] Mitra M., Kulsi C., Kargupta K., Ganguly S., Banerjee D., Composite of polyaniline bismuth selenide with enhanced thermoelectric performance, *J. Appl. Polym. Sci*., 135, 46887, **2018**.

[20] Holla S., Selvakumar M., Effect of Different Electrolytes on the Supercapacitor Behavior of Single and Multilayered Electrode Materials Based on Multiwalled Carbon Nanotube/Polyaniline Composite, *Macromol. Chem. Phys.*, 219, 1870048, **2018.**

[21] Li P., Zhang D., Xu Y., Ni C., Shi G., Sang X., Cong H., Hierarchical porous polyaniline supercapacitor electrode from polyaniline/silica self aggregates, *Polym. Int*, 67, 1670-1676, **2018**.

[22] Li Z., Hu J., Li Y., Liu J., Ce3+Doped Polyaniline Hollow Microspheres as Electrode Material of Supercapacitor, *Chemistry Select*, 3, 6737-6742, **2018.**

[23] Liu Y., Zhang B., Xu Q., Hou Y., Seyedin S., Qin, S., Wallace G.G., Beirne S., Joselito M.R., Chen J., Development of Graphene Oxide/Polyaniline Inks for High Performance Flexible Microsupercapacitors via Extrusion Printing, *Adv. Funct. Mater.*, 22, 1870142, **2018.**

[24] Ran F., Tan Y.T., Dong W.J., Liu Z., Kong L.B., Kang L., In situ polymerization and reduction to fabricate gold nanoparticle-incorporated polyaniline as supercapacitor electrode materials, *Polym. Adv. Technol.*, 29, 1697-1705, **2018**.

[25] Tan Y.T., Zhang Y.F., Kong L.B., Kang L., Ran F., Nano-Au@PANI core-shell nanoparticles via in-situ polymerization as electrode for supercapacitor, *J. Alloys. Compd*., 722, 1-7, **2017.**

[26] Tan Y.T., Liu Y.S., Zhang Y.F., Xu C.G., Kong L.B., Kang L., Ran F., Dulse-derived porous carbon–polyanilinenanocomposite electrode for high-performance supercapacitors, *J. Appl.Polym. Sci.*, 135, 45776, **2018.**

[27] Frisch M., et al. Gaussian 09 Revision C.01, Gaussian Inc., *Wallingford CT*, **2010**.

[28] Becke A.D., Density-functional thermochemistry. III. The role of exact exchange, *Chem. Phys.*, 98, 5648-5652, **1993.**

[29] Lee C., Yang W., Parr R.G., Development of the Colle-Salvetti correlation-energy formula into a functional of the electron density, *Phys. Rev. B.*, 37, 785-789., **1988.**

[30] Miehlich B., Savin A., Stoll H., Preuss H., Results obtained with the correlation energy density functionals of becke and Lee, Yang and Parr, *Chem. Phys. Lett*., 157, 200-206, **1989.**

[31] Ibrahim M., El-Haes H., Computational Spectroscopic Study of Copper, Cadmium, Lead and Zinc Interactions in the Environment, *Int. J. Environment and Pollution*, 23, 4, 417-424, **2005.**

[32] Ibrahim M., Mahmoud A.A., Computational Notes on the Reactivity of some Functional Groups, *J. Comput. Theor. Nanosci*., 6, 1523-1526, **2009.**

[33] Politzer P., Laurence P.R., Jayasuriya K., Molecular Electrostatic Potentials: An Effective Tool for the Elucidation of Biochemical Phenomena, *Environ. Health Persp.*, 61, 191-202, **1985.**

[34] Politzer P., Murray J.S., Molecular Electrostatic Potentials: Concepts and Applications, *J Theor. Comput. Chem*, 3, 649, **1996.**

[35] Ezzat H., Badry R., Yahia I.S., Zahran H.Y., Elhaes H., Ibrahim M.A., Mapping the molecular electrostatic potential of carbon nanotubes, *Biointerface Research in Applied Chemistry*, 8, 3539-3542, **2018.**
[36] Ammar N.S., Elhaes H., Ibrahim H.S., El-hotaby W., Ibrahim M.A., A Novel Structure for Removal of Pollutants from Wastewater, *Spectrochim Acta A*, 121C, 216-223**, 2014.**
[37] Ibrahim M., Saleh N.A., Elshemey W.M., Elsayed A.A., Hexapeptide Functionality of Cellulose as NS3 Protease Inhibitors, *Medicinal Chemistry*, 8, 826-830, **2012.**
[38] Ibrahim M., Osman O., Spectroscopic Analyses of Cellulose: Fourier Transform Infrared and Molecular Modelling Study, *J. Comput. Theor. Nanosci.*, 6, 1054–1058, **2009.**
[39] Dedkov Y., Voloshina E., Spectroscopic and DFT studies of graphene intercalation systems on metals, *J. Electron. Spectrosc.*, 219, 77-85, **2017**.
[40] Üngördü A., Tezer N., DFT study on metal-mediated uracil base pair complexes, *J. Saudi Chem. Soc.*, 21(7), 837-844, **2017**.
[41] Khoutoul M., Lamsayah M., Al-blewi F. F., Rezkib N., Aouad M. R., Mouslim M., Touzani R., Liquid–liquid extraction of metal ions, DFT and TD-DFT analysis of some 1,2,4-triazole Schiff Bases with high selectivity for Pb(II) and Fe(II), *J. Mol. Struct.*, 1113, 99-107, **2016**.
[42] Fischer M., DFT-based evaluation of porous metal formates for the storage and separation of small molecules, *Micropor. Mesopor. Mat.*, 219, 249-257, **2016**.
[43] Wang W., Fan L., Wang G., Li Y., CO_2 and SO_2 sorption on the alkali metals doped CaO(100)surface: A DFT-D study, *Appl. Surf. Sci.*, 425, 972-977, **2017**.